RSC Advances

This is an *Accepted Manuscript*, which has been through the Royal Society of Chemistry peer review process and has been accepted for publication.

Accepted Manuscripts are published online shortly after acceptance, before technical editing, formatting and proof reading. Using this free service, authors can make their results available to the community, in citable form, before we publish the edited article. This *Accepted Manuscript* will be replaced by the edited, formatted and paginated article as soon as this is available.

You can find more information about *Accepted Manuscripts* in the **Information for Authors**.

Please note that technical editing may introduce minor changes to the text and/or graphics, which may alter content. The journal's standard **Terms & Conditions** and the **Ethical guidelines** still apply. In no event shall the Royal Society of Chemistry be held responsible for any errors or omissions in this *Accepted Manuscript* or any consequences arising from the use of any information it contains.

ARTICLE TYPE

Nanocomposite coatings with stimuli-responsive catalytic activity[†]

Meike Koenig,[a,b] David Magerl,[c] Martine Philipp,[c] Klaus-Jochen Eichhorn,[a] Martin Müller,[a] Peter Müller-Buschbaum[c], Manfred Stamm[a,b] and Petra Uhlmann[*a]

Stimuli-responsive catalytic coatings are fabricated by *insitu*-synthesis of metallic nanoparticles in binary PNIPAM-P2VP (poly(N-isopropyl acrylamide)-poly(2-vinyl pyridine)) brushes. The amount of immobilized nanoparticles is found to be controllable by the polymer ratio, since solely P2VP interacts with the nanoparticles. The *insitu*-synthesis of nanoparticles is studied by attenuated total reflection Fourier transform infrared spectroscopy and atomic force microscopy, whereas the swelling behavior of the polymer films is investigated by spectroscopic ellipsometry and grazing incidence small angle X-ray scattering. Temperature dependent catalytic activity is probed by use of the reduction of nitrophenol to aminophenol as a model reaction. Control of the catalytic activity by the temperature induced deswelling of PNIPAM is observed.

1 Introduction

The development of smart stimuli-responsive surface coatings has been the subject of many investigations over the last years. Especially, so-called polymer brushes are regarded as very promising candidates.[1,2] Polymer brushes consist of polymer chains tethered by one end to a planar or curved substrate in close proximity to each other so that the chains are forced to stretch away from the surface in a brush conformation.[3] Depending on the nature of the polymer, these systems are capable of responding to external stimuli such as temperature, solvent polarity and pH, generally by reversible swelling-deswelling behavior. Furthermore, surface coatings with complex swelling behavior can be created by grafting of mixed polymer brushes,[4] and accessible functional groups can be used to immobilize nanoscopic moieties such as nanoparticles or biomolecules. The combination with the unique properties of the immobilized moieties offers new applications for polymer brushes in sensors, medicine and catalysis. Such use of polymer brushes as carrier systems for nanoparticles has been the subject of several scientific reports during recent years.[5–8] We immobilized nanoparticles in polymer brushes either by covalent or non-covalent interactions and either with functional groups along the whole chain or at specific endgroups of the polymer chain.s[9–11] Additionally, polymer brushes have been used as "nanoreactors" where nanoparticles can be formed *insitu* and both immobilized and stabilized on the surface simultaneously.[12] In a previous report, we investigated the use of P2VP mono brushes as a template for the formation of catalytically active palladium or platinum nanoparticles.[13]

Due to their stimuli-responsive swelling behavior, such polymer brushes cannot only be used as sole carriers but also to modulate the properties of the immobilized moieties.[2] For example, we could affect the surface plasmon resonance peak of nanoparticles immobilized on solvent sensitive polystyrene brushes[10] or on pH sensitive P2VP brushes.[12] These systems show promising properties applicable in sensor systems. The fabrication of stimuli-responsive catalytic systems, which allow the control of the catalytic activity by changes in the environment, has been investigated by several groups so far, mostly by exploiting microgels.[14–17] Up to now, only the use of spherical polymer brushes, i. e. polymer brushes grafted to a curved substrate, e. g. latex particles, has been reported for stimuli-responsive catalytic systems.[18,19] To the best of our knowledge, no reports on the fabrication of stimuli-responsive catalytic coatings on macroscopic surfaces have been reported by now. Immobilization of catalysts on macroscopic surfaces eases the reuse and recycling of precious catalyst and renders promising candidates for lab-on-a-chip-systems and novel smart coatings for micro reaction technology or chemical engineering.

In the present article, we report on the fabrication of such coatings by *insitu*-synthesis of Pd and Pt nanoparticles in bi-

a Leibniz-Institut für Polymerforschung Dresden e.V., Hohe Straße 6, 01069 Dresden, Germany. Fax: 49 351 4658281; Tel: 49 351 4658236; E-mail: uhlmannp@ipfdd.de
b Technische Universität Dresden, Zellescher Weg 19, 01062 Dresden,Germany.
c Technische Universität München, Physik-Department, Lehrstuhl für Funktionelle Materialien, James-Franck-Straße 1, 85748 Garching, Germany.

RSC Advances Accepted Manuscript

nary PNIPAM-P2VP brushes (Figure 1). The interaction of the nanoparticles with the polymer has been investigated, as well as the influence of the incorporated nanoparticles on the responsive swelling behavior of the polymer brushes. Via a well-known model reaction, the reduction of 4-nitrophenol to 4-aminophenol,[20–22] the temperature dependent catalytic activity has been studied.
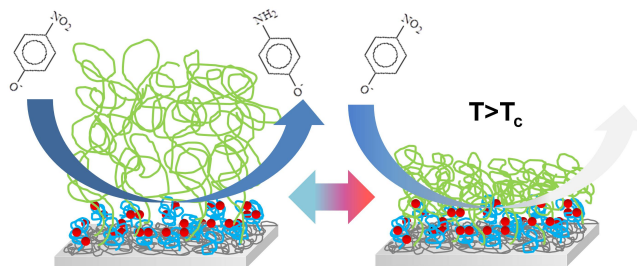
Fig. 1 Scheme of stimuli-responsive catalysis of nanoparticles in binary polymer brushes; the temperature induced phase transition of PNIPAM chains (green) at T_c is proposed to lead to a diffusional barrier blocking the access of the reactants to the catalyst

2 Experimental

Materials: Poly (glycidyl methacrylate) (PGMA, M_n= 17 500 g/mol, M_w/M_n=1.7), carboxyterminated poly(2-vinyl-pyridine) (P2VP40,6k: M_n= 40 600 g/mol, M_w/M_n=1.08; and P2VP10k:M_n= 10 000 g/mol, M_w/M_n=1.08) and carboxy-terminated poly(N-isopropylacrylamide) (PNIPAM47,6k: M_n= 47 600 g/mol, M_w/M_n=1.22 and PNIPAM56k: M_n= 56 000 g/mol, M_w/M_n=1.4) were purchased from Polymer Source, Inc., Canada. Hexachloroplatinic acid hexahydrate (H_2PtCl_6 ·$6H_2O$), palladium chloride ($PdCl_2$), sodium borohydride ($NaBH_4$), sodium acetate($NaC_2H_3O_2$) and 4-nitrophenol ($C_6H_5NO_3$) were purchased from Aldrich, Germany. Ammonium hydroxide (NH_4OH) was purchased from Acros, Germany. Ethanol abs. was purchased from VWR, Germany. Chloroform ($CHCl_3$) was purchased from Fisher, Germany. Hydrogen peroxide (H_2O_2) and Acidic acid ($C_2H_4O_2$) were purchased from Merck, Germany. All chemicals were used as received. Highly polished single-crystal silicon wafers of {100} orientation with ca. 1.5 nm thick native silicon oxide layers were purchased from Silicon Materials, Inc. (USA) and used as substrates. Millipore water purified with Purelab Plus Ⓡ ultrapure, was employed throughout experiments.

Instrumentation: The thickness of layers was measured on a SE400adv ellipsometer (SENTECH Instruments GmbH, Berlin, Germany) as described elsewhere.[23] *Insitu* SE measurements were performed with an alpha-SE (Woollam Co.,

Inc., Lincoln NE, USA), equipped with a rotating compensator, within a batch cuvette (TSL Spectrosil, Hellma, Muellheim, Germany).[24] All measurements were performed in the spectral region 370-900 nm at an angle of incidence of 70°. AFM studies were performed with a Dimension 3100 (Digital instruments, Inc., Santa Barbara, USA) microscope. Tapping mode was used to map the film morphology at ambient conditions. ATR-FTIR spectra were recorded with a IFS55 spectrometer (Bruker Optics GmbH, Leipzig, Germany) using the "single-beam-sample-reference" method (OPTISPEC, Zürich, Switzerland). UVvis spectra were taken with a Specord40 spectrometer (Analytik Jena, Jena, Germany). Grazing incidence small angle x-ray scattering (GISAXS) measurements were performed at the beamline BW4 of the DORIS III storage ring at DESY in Hamburg, Germany.

Preparation of binary polymer brushes: Binary PNIPAM-P2VP brushes were prepared by the "grafting to" method on silicon substrates as it has been described earlier.[25] The silicon wafers were first cleaned by treating them for 30 min in a 1:1:5 mixture of 30% hydrogen peroxide, 29% ammonium hydroxide and water at 75 °C. Then they were rinsed several times with water. A layer of PGMA was spin-coated onto the wafers from a 0.02 wt-%-solution in chloroform and then annealed for 10 min at 110 °C. Onto that anchoring layer first P2VP-chains were grafted in low density by spin-coating from a P2VP solution in chloroform (0.0125-0.05 wt-%) and subsequent annealing for 3 h at 150 °C. Ungrafted polymer was extracted by chloroform. In a second step PNIPAM chains were grafted to the anchoring layer by spin-coating from a 1 wt-% solution in chloroform and annealing at 175 °C overnight. Ungrafted polymer was again extracted by chloroform. Binary brushes with various constitutions were prepared. The process was traced by ellipsometry in dry state. For AFM studies P2VP40,6k and PNIPAM47,6k and for ATR-FTIR and GISAXS P2VP40,6k and PNIPAM56k were used, all other experiments were done with P2VP10k and PNIPAM56k.

Preparation of nanoparticles in polymer brushes: Pd or Pt nanoparticles were formed *insitu* in binary polymer brushes. Therefore, metal ions (Pd^{2+} or $PtCl_6^{2-}$) were adsorbed to the polymer out of the solution of the corresponding metal salt. A polymer brush-coated wafer was stirred in a solution of $PdCl_2$ in ethanol (0.14 mM) or H_2PtCl_6 in water (2mM) for several minutes (Pd: 5 min, Pt: 300 min) and rinsed with ethanol. For reduction to nanoparticles the sample was put in a freshly prepared 0.2 M aqueous solution of $NaBH_4$ (Pd: 120 min, Pt: 5 min) and finally rinsed with ethanol.

Catalysis of 4-Nitrophenol-Reduction:A polymer brush-coated wafer (1x3 cm) with immobilized nanoparticles was put in a PMMA cuvette with 2 ml of a 0.2 mM solution of

4-nitrophenol in water. Before and after the catalysis experiment the solution was found to be at pH 9. The cuvette was heated or cooled to the desired temperature by a water bath and equilibrated at that temperature for several minutes. To start the reaction 1 ml of 20 mM NaBH$_4$-solution was added. UVvis spectra were taken every 200 s. For each temperature a new wafer of the same nanoparticle-batch was used.

Spectroscopic Ellipsometry Data Modeling: An optical box model consisting of multiple layers (Si, SiO$_2$, PGMA and polymer brush) was used to evaluate ellipsometry measurements. For dry measurements, the modifications with polymer layers were modeled with a fixed refractive index (n$_{PGMA}$=1.525, n$_{P2VP}$=1.595, n$_{P2VP+PNIPAM}$=1.545). For *in-situ* measurements, a two-parameter Cauchy dispersion model was used to determine both refractive index and thickness of the swollen polymer brush layer. By the use of a three-component effective medium approach (EMA) the volume fractions of the components were determined using the P2VP index of refraction and literature values of the dielectric functions of Pd or Pt.[26]

GISAXS Measurements and Modeling: To measure the structural changes in PNIPAM-P2VP brushes with and without nanoparticles, the samples were immersed in the respective solution at the desired temperature for 5 min and dried thereafter. GISAXS measurements were performed with an x-ray wavelength of 0.138 nm. For all experiments the angle of incidence of the x-ray beam onto the sample surface was fixed to 0.5°. A sample-detector distance of 2116 mm was chosen and a two dimensional (2D) detector MarCCD from Mar Research (2048 × 2048 pixel) was utilized. These chosen settings allow covering a q_y-range from 0.001 to 2 nm^{-1}. The specular peak was blocked by a point-shaped beamstop. The coordinate system for describing the GISAXS experiment is defined as follows: the z-axis is oriented perpendicular to the sample surface and the (x,y)-plane is given by the sample surface with the x-axis being oriented in the direction of the incident x-ray beam. The components of the scattering vector q are given by:

$$q_x = \frac{2\pi}{\lambda}\left[\cos\psi\cos\alpha_f - \cos\alpha_i\right] \qquad (1)$$

$$q_y = \frac{2\pi}{\lambda}\left[\sin\psi\cos\alpha_f\right] \qquad (2)$$

$$q_z = \frac{2\pi}{\lambda}\left[\sin\alpha_i - \sin\alpha_f\right] \qquad (3)$$

where α_i and α_f denote the incident and exit angles of the x-ray beam. The scattering plane is the (x,z)-plane and defined by the incident and exit angles. Scattering out of this plane is probed under an out-of-plane angle ψ. Further details of the theoretical background of GISAXS and the used setup are given in the references.[27–29] A quantitative analysis of the out-of-plane line cuts of the 2D GISAXS data is provided in

the frame of the distorted wave Born approximation[27,30,31] using the local monodisperse approximation (LMA) and a model of cylindrical objects having a Gaussian size distribution arranged on a one-dimensional paracrystal.[32]

3 Results and discussion

The formation of nanoparticles on a surface functionalized with polymer brushes was examined with various techniques. Attenuated total reflection Fourier transform infrared (ATR-FTIR) spectra were recorded to investigate the interaction of the metal precursors with the polymer chains. Figure 2 shows the spectra of PNIPAM-P2VP brushes before and after the adsorption of Pd^{2+} together with the spectra of the mono brushes for comparison. The spectrum of the binary brush combines the features of the spectra of the mono brushes in this spectral range, with the amide bands at 1550 and 1645 cm^{-1} assigned to PNIPAM and the ring vibrations of the pyridine group at 1475, 1570 and 1590 cm^{-1} assigned to P2VP. Interestingly, compared to the spectra of the mono brushes, the amide I band at 1550 cm^{-1} is upshifted and the pyridine band at 1475 cm^{-1} is downshifted for the binary brush, probably owing to interactions between the two polymers. Upon adsorption of Pd^{2+}, the amide bands remain in their former shape and position, whereas two of the pyridine bands are shifted to higher wavenumbers (1480 and 1605 cm^{-1}),[33] which has also been observed for experiments with P2VP mono brushes.[13] Coordination of Pd^{2+} to the free electrons of the pyridine-nitrogen increases the order of the C=C- and C=N-bonds resulting in the observed shift. Since no shift of the amide bands is detected, no complexation of Pd^{2+} by the amide groups of PNIPAM can be observed.[34]

Just as well, no nanoparticles can be detected in atomic force microscopy (AFM) images of the surface of PNIPAM mono brushes, treated the same way as P2VP mono brushes, although these show complete coverage of the surface with nanoparticles (Figure 3). A reason for this might be the formation of a tight physical network between closely tethered PNIPAM chains via hydrogen bonds between the amide groups. PNIPAM brushes were also found to be resistant against adsorption of proteins.[35] Corresponding to these findings, the coverage of the surface with nanoparticles increases with higher P2VP content in the binary brush (Figure 3), shown here for Pt nanoparticles. Pd nanoparticles were found to behave in the same manner. Similar experiments for synthesis of nanoparticles in P2VP studied with TEM, revealed the actual size of the nanoparticles to be 1 nm and 2 nm for palladium and platinum nanoparticles, respectively.[13]

The presented studies reveal that Pd and Pt nanoparticles can be synthesized *insitu* in PNIPAM-P2VP brushes via interaction with the pyridine group of P2VP. The amount of
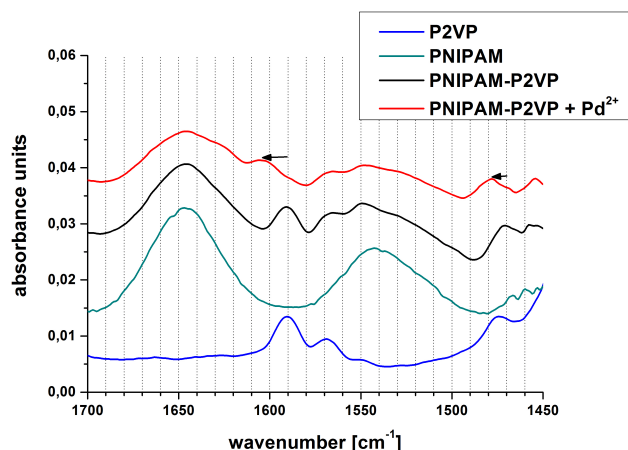
Fig. 2 ATR-FTIR Spectra of mono P2VP and PNIPAM brushes and binary PNIPAM-P2VP-brushes (PNIPAM56k-P2VP40,6k, 60:40) with and without adsorbed Pd^{2+}; spectra were shifted along the vertical axis for better display, the arrows indicate the observed shift in the spectrum with Pd^{2+}

nanoparticles on the surface can be controlled by the composition of the binary brush.

To gain a high grafting density of the temperature-sensitive component PNIPAM and a high coverage of the surface with catalytically active nanoparticles at the same time, binary brushes with a low molecular weight P2VP component (10 000 g/mol) were prepared and used for most of our studies (see experimental). The small chain length allows the grafting of P2VP in a high density, while at the same time constituting a lower diffusional barrier for the grafting of PNIPAM as a second brush polymer. Comparative SEM studies revealed that the influence of the chain length on the nanoparticle formation is of minor importance.†

3.1 Stimuli-Responsive Swelling

To investigate the influence of the incorporation of nanoparticles on the responsive swelling behavior of the polymer brushes spectroscopic ellipsometry(SE) and grazing incidence small angle X-ray scattering (GISAXS) experiments were conducted. The temperature dependent swelling was monitored via *insitu*-SE. PNIPAM is well known for its temperature sensitive behavior showing a phase transition at $T_c \sim 32\,^{\circ}C$ in pure water.[36] Experimental SE data acquired in the spectral region of 370-900 nm were modeled with a stratified layer optical model, comprising four layers which account for the silicon substrate, the SiO_2-layer, the anchoring layer and the polymer brush, respectively. The wavelength dependence of the effective refractive index of the polymer brush layer with immobilized nanoparticles swollen in water at pH 7 could be
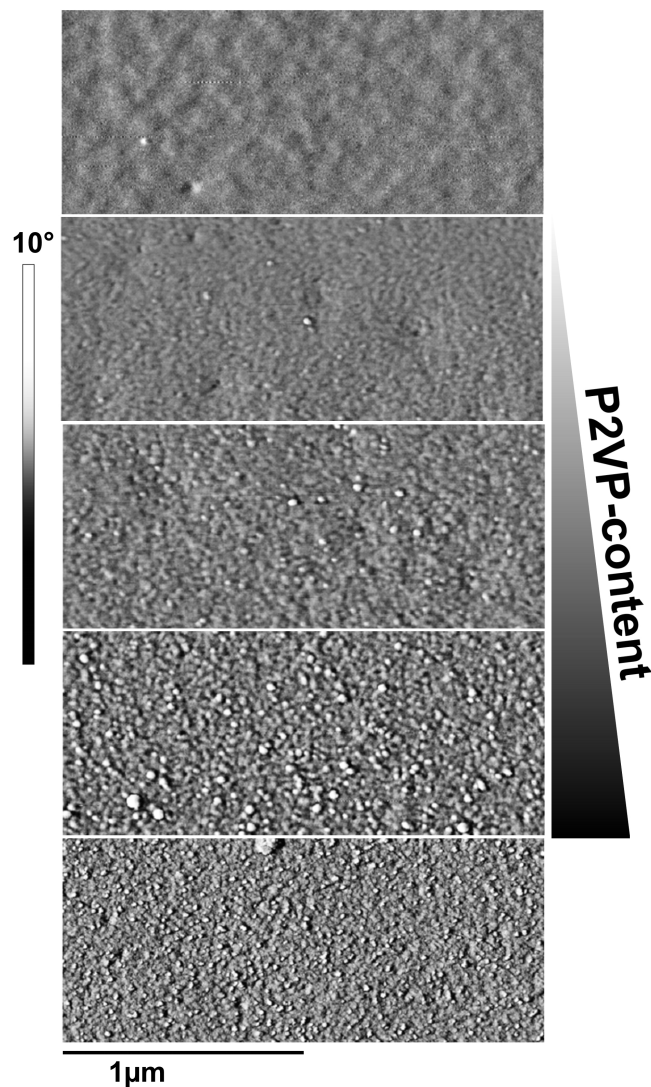
Fig. 3 AFM phase images of polymer brushes with increasing P2VP content after the immobilization of Pt nanoparticles (from top to bottom: PNIPAM mono brushes (47,6k)- PNIPAM-P2VP(85:15), PNIPAM-P2VP(75:25), PNIPAM-P2VP(65:35), P2VP mono brushes (40,6k)

a)

b)
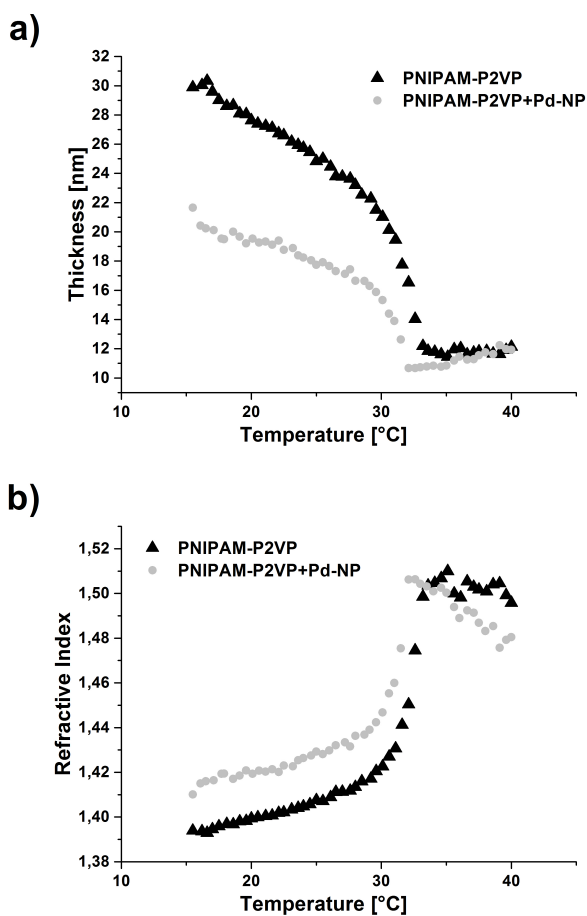
Fig. 4 Temperature responsiveness of PNIPAM-P2VP brushes (PNIPAM56k-P2VP10k, 60:40) with and without Pd nanoparticles determined from SE measurements (a) thickness, b) refractive index

20°C - pH7   40°C - pH3

Drying

Fig. 5 Schematic of the proposed changes in the lateral structure of PNIPAM-P2VP brushes in swollen and dry state upon treatment with two different ambient conditions; green: PNIPAM, blue: P2VP

described with a normal Cauchy dispersion lineshape. A three component effective medium approach (EMA) consisting of water, polymer and metal gave a volume percentage of only $\sim 1\%$ for the nanoparticles, since the P2VP component of the brush, where the nanoparticles are localized, does not swell under the applied neutral conditions and remains near the surface of the substrate.

Figure 4 shows the best-match model thickness and refractive index of binary PNIPAM-P2VP brushes with and without nanoparticles dependent on temperature. The polymer brushes exhibit a first slowly than abruptly declining thickness between 20 °C and 32 °C where the brushes collapse to nearly their dry thickness of ~ 10 nm. The phase transition occurs in a broader region than known from PNIPAM in solution[36,37] and thin films,[38-40] which is a common behavior for grafted polymers.[41-43] After the immobilization of nanoparticles the thickness of the swollen polymer brush is reduced,

and the position of T_c is slightly shifted to lower temperatures. Both effects are assigned to a slight decrease of the PNIPAM grafting density,[44] during the formation of nanoparticles under basic conditions, which can lead to the cleavage of the ester bond to the anchoring layer. After nanoparticle formation, the thickness of the dry polymer layer was found to have decreased by 4 nm, as well. For Pt nanoparticles, where the reduction time is shorter, no decrease in thickness of the dry and swollen brushes had been found. *Insitu*-AFM measurements of the swelling at 20 °C by razor cuts confirmed the results modeled from SE data.†

Binary brushes exhibit a characteristic swelling behavior upon treatment with a selective solvent, where lateral ("ripple") or perpendicular ("dimple") phase separation occurs.[45,46] If the solvent is removed very fast, these phases can be frozen in and identified also in the dry state. Figure 5 displays the proposed lateral changes in the binary brushes for two different ambient conditions. At 20 °C and pH 7 only PNIPAM is swollen, while P2VP is in a collapsed state. The contrary state is found at the conditions of 40 °C and pH 3, where water is a selective solvent for the now strongly positively charged P2VP, and PNIPAM is collapsed. By means of GISAXS the structural changes occurring during switching of the binary PNIPAM-P2VP brushes with and without nanoparticles were probed in dependence of pre-treatment with solutions of different temperature and pH.

The lateral changes are quantified using GISAXS. Horizontal line cuts (with respect to the sample surface) of the 2D GISAXS data at the position of the Yoneda peak of the polymers yield this information.[27] The error of the values indi-
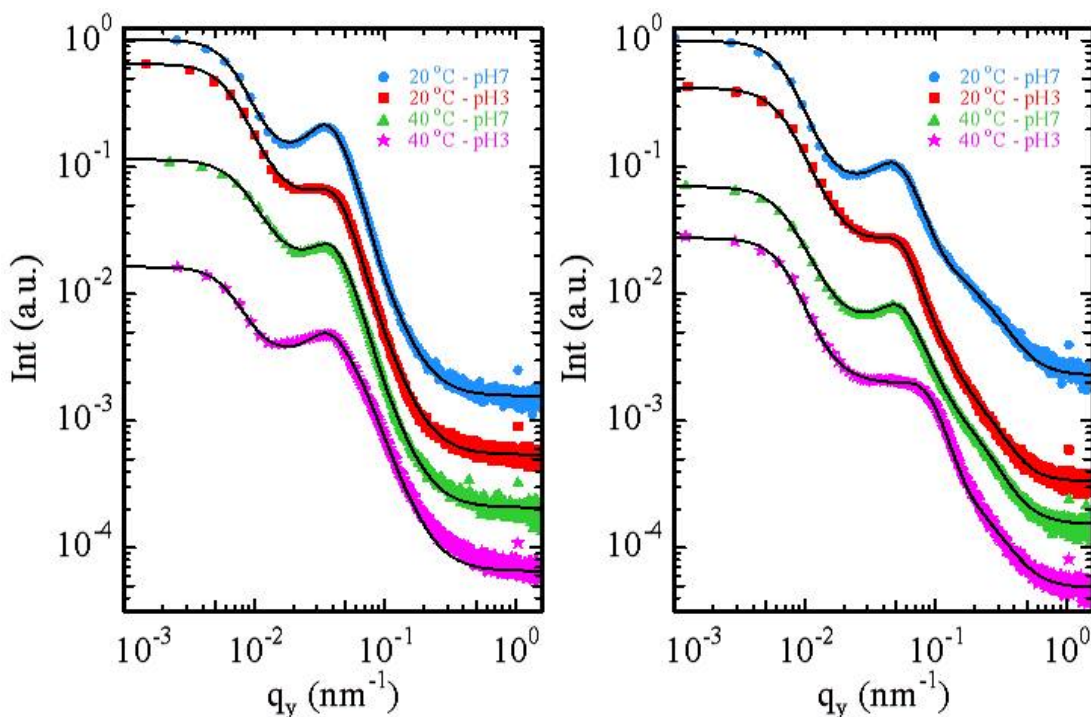
Fig. 6 Horizontal line cuts of 2D GISAXS data (symbols) and fits (lines) based on the model as described in the text for the binary PNIPAM-P2VP brush (PNIPAM56k-P2VP40,6k, 70:30) without(a) and with (b) Pd nanoparticles. The conditions are (top to bottom): 20 °C, pH 7 ; 20 °C, pH 3; 40 °C, pH 7 and 40 °C, pH 3; curves were shifted vertically for clarity of presentation

cated below, is between 5 and 10 %. According to Figure 6(a), at 20 °C and pH 7 for the PNIPAM-P2VP brush one characteristic peak-like feature, positioned at about $q_y = 0.06$ nm^{-1}, is observed in the GISAXS data. The fitting of the horizontal line cuts with the model given in the Experimental Section, provides a structure factor with a size of 125 nm. It is attributed to the average center-to-center distance between the dimples,[31] which are formed within the micro-phase separated binary brush. The average radius of the dimples is of about 31 nm for this brush. The dimple structure of the binary brush with Pd nanoparticles possesses smaller characteristic sizes at 20 °C and pH 7: the average center-to-center distance of the dimples is 85 nm and their average radius is 25 nm (see Figure 6(b)). However, the horizontal line cut of the 2D GISAXS data of the brush with Pd nanoparticles shows in addition a broad shoulder located at 0.3 nm^{-1}. This shoulder is attributed to 8 nm large agglomerates of Pd nanoparticles present in the P2VP brush component. All of these structural characteristics agree well with the local observations based on the AFM data.† Therefore the AFM data give representative topography information and no additional inner structures are present in the brushes.

The horizontal line cuts depicted in Figure 6(a) show that the switching of the binary brush without nanoparticles re-

sults in a considerable change of its dimple structure. As expected, the largest lateral structural changes of the brush happen when varying between the conditions 20 °C pH 7 and 40 °C pH 3. The radius of the dimples actually decreases from 31 to 18 nm upon switching from 20 °C and pH 7 to the conditions 40 °C and pH 3, and the center-to-center distance of the dimples is reduced from 125 to 110 nm. Both structure and form factor of the dimples are systematically larger in case of the PNIPAM-P2VP without nanoparticles as compared to the binary brushes containing nanoparticles. Figure 6(b) confirms that the switching of the binary brush with Pd nanoparticles as function of temperature and pH modifies its dimple structure in a similar way as for the binary brush without nanoparticles. The radius of the dimples indeed decreases from 25 to 16 nm, and the average center-to-center distance decreases from 85 to 52 nm. For the PNIPAM-P2VP brush with Pt nanoparticles, a similar switching behavior of the dimple structure is also observed in dependence of pH and temperature. This proves that the functional characteristics of the polymer brushes, their stimuli-responsive behavior, is still present after the immobilization of nanoparticles.

3.2 Stimuli Responsive Catalytic Activity

The catalytic activity of the nanoparticles in the brush was tested by the reduction of 4-nitrophenol with $NaBH_4$. This reaction can easily be monitored by UVvis-spectroscopy[20–22] and has therefore been chosen as a model reaction. Since 4-nitrophenol shows a characteristic absorption band at 400 nm, whereas 4-aminophenol characteristically absorbs at 300 nm, the rate of the reduction can be determined by the decrease of the absorbance at 400 nm. The reaction was performed directly inside the spectrometer with the catalyst wafer fixed at the side of the cuvette. For temperature dependent measurements the cuvette with the sample was kept at a specific temperature for several minutes. To start the reaction, a given volume of $NaBH_4$-solution was added to the 4-nitrophenol-solution. The color of the solution changed immediately to a deep yellow, since addition of $NaBH_4$ results in an increase of pH and the hydroxyl groups of the phenol get deprotonated.[20] In the UVvis spectra taken consecutively every 200 s, the absorbance at 400 nm decreases with time and a new absorption band at 300 nm appears (Figure 7a). For nanoparticles in binary PNIPAM-P2VP brushes, especially the variance of the reaction rate with temperature was investigated. According to Arrhenius,[47] for a simple thermally activated process, $\ln k$ is expected to decrease linearly with $1/T$ according to

$$\ln k_{app} = -\frac{E_A}{k_B T} \qquad (4)$$

(k_{app}: apparent rate constant, E_A: activation energy, k_B: Boltzmann constant, T: absolute temperature)

Figure 7b shows the Arrhenius plot for the reduction of 4-nitrophenol with $NaBH_4$ using Pd nanoparticles in P2VP brushes and PNIPAM-P2VP brushes as catalysts. A similar catalytic behavior was found for Pt nanoparticles, although the rate constant was found to be overall lower, since less nanoparticles were immobilized. As expected, nanoparticles in P2VP brushes exhibit normal Arrhenius-like behavior and the rate constant increases with temperature. It has to be clarified that the absolute reaction rate in between the P2VP and the binary brushes cannot be compared since the amount of nanoparticles present on the P2VP brushes was less. Therefore, only the trend in the reaction rate with temperature is discussed here. For the nanoparticles in binary brushes, data of three batches of the nanoparticle synthesis are shown, where for each temperature, a new sample was used. Due to slight variations in the amount of immobilized nanoparticles in between the different batches, a slight difference in the absolute catalytic activity was found at the same temperature. Nevertheless, all three batches displayed a similar trend in catalytic activity, exhibiting a deviation from normal Arrhenius-like behavior: in the region between 20 °C and 32 °C where the polymer brush shows a declining thickness, the reaction
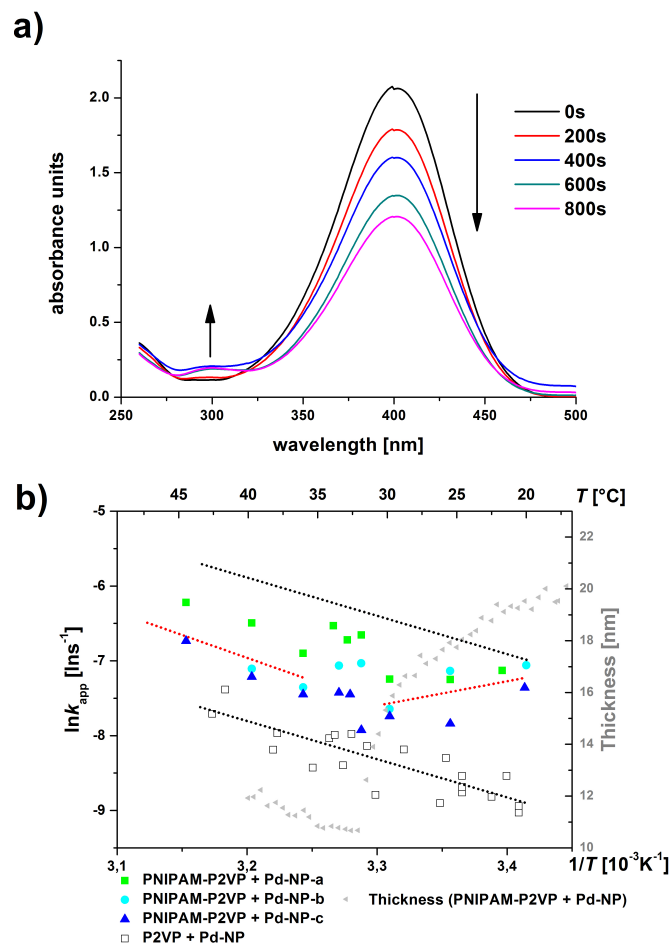
Fig. 7 Reduction of 4-nitrophenol to 4-aminophenol catalyzed by Pd nanoparticles in PNIPAM-P2VP brushes (PNIPAM56k-P2VP10k, 60:40); (a) change in absorption spectra over time, (b) temperature dependence of the reaction rate compared to catalysis by Pd nanoparticles in P2VP brushes (each type of symbol represents one batch of samples) and swollen thickness (SE data); dotted lines were inserted to serve as a guide to the eye, the red line indicating deviation from Arrhenius-like behavior

rate slightly decreases with temperature. In this region, the effect of temperature on the reaction rate is overcompensated by the influence of the increasing diffusional barrier of the collapsing PNIPAM chains. At the phase transition, a sudden increase in the reaction rate is detected. Above 32 °C where the thickness of the polymer layer remains more or less constant, solely temperature affects the reaction rate and therefore an Arrhenius-like behavior of the reaction rate can be detected. It is encouraging that this effect of the diffusional barrier was detected, regardless of the small size of the reactants in the used model reaction.

4 Conclusions

Novel catalytic coatings with stimuli-responsive catalytic activity were fabricated by *insitu* synthesis of metallic nanoparticles in PNIPAM-P2VP binary brushes. The collapse of PNIPAM chains with increasing temperature creates a diffusional barrier for the reactants, resulting in a decreased reaction rate in comparison to the trend observed for the catalysis with nanoparticles in mono P2VP brushes. These novel coatings therefore show non-Arrhenius like catalytic activity. The responsive swelling of polymer brushes with immobilized nanoparticles is detected by SE and GISAXS. ATR-FTIR spectra demonstrated that the metallic precursor only interacts with the P2VP component of the polymer brush, while the spectral features assigned to PNIPAM remained unchanged. Just as well, AFM studies showed no immobilization of nanoparticles in PNIPAM mono brushes and an increasing nanoparticle content with increasing P2VP-portion in the binary brush. Therefore, the content of nanoparticles can be controlled by the polymer ratios. Further tuning of the temperature responsive effect is expected via adjustment of the chain length and grafting density of the temperature sensitive component PNIPAM or the choice of a different model reaction with reactants with lower diffusion constant. Even catalytic systems stimulated by different physical effects, such as light or electric current, can be fashioned since the use of the "grafting to" approach allows for the easy preparation of various mixed brush systems. In summary, the *insitu* synthesis of nanoparticles in mixed polymer brushes provides a facile way to create interesting novel coatings with stimuli-responsive properties, applicable in novel sensor systems and smart catalytic devices.

5 Acknowledgments

References

1   M. A. Cohen Stuart, W. T. Huck, J. Genzer, M. Müller, O. Christopher, M. Stamm, G. Sukhorukov, I. Szleifer, V. V. Tsukruk, M. Urban, F. Winnik, S. Zauscher, I. Luzinov and S. Minko, *Nat. Mater.*, 2010, **9**, 101.
2   O. Azzaroni, *J. Polym. Sci. A1*, 2012, **50**, 3225.
3   W. J. Brittain and S. Minko, *J. Polym. Sci. A1*, 2007, **45**, 3505.
4   S. Minko, D. Usov, E. Goreshnik and M. Stamm, *Macromol. Rapid Commun.*, 2001, **22**, 206.
5   R. A. Gage, E. P. Currie and M. A. Cohen Stuart, *Macromolecules*, 2001, **34**, 5078.
6   Z. Liu, K. Pappacena, J. Cerise, J. Kim, C. J. Durning, B. O'Shaughness and R. Levicky, *Nano Lett.*, 2002, **2**, 219.
7   C.-W. Chen, M.-Q. Chen, T. Serizawa and M. Akashi, *Adv. Mater.*, 1998, **10**, 1122.
8   G. Sharma and M. Ballauff, *Macromol. Rapid Commun.*, 2004, **25**, 547.
9   S. Gupta, M. Agrawal, P. Uhlmann, F. Simon and M. Stamm, *Chem. Mater.*, 2010, **22**, 504.
10 S. Gupta, M. Agrawal, P. Uhlmann, F. Simon, U. Oertel and M. Stamm, *Macromolecules*, 2008, **41**, 8152.
11 S. Gupta, P. Uhlmann, M. Agrawal, V. Lesnyak, N. Gaponik, F. Simon, M. Stamm and A. Eychmüller, *J. Mater. Chem.*, 2008, **18**, 214.
12 S. Gupta, P. Uhlmann, M. Agrawal, S. Chapuis, U. Oertel and M. Stamm, *Macromolecules*, 2008, **41**, 2874.
13 M. Koenig, F. Simon, P. Formanek, M. Müller, S. Gupta, M. Stamm and P. Uhlmann, *Macromol. Chem. Phys.*, 2013, **214**, 2301.
14 C.-W. Chen, K. Arai, K. Yamamoto, T. Serizawa and M. Akashi, *Macromol. Chem. Phys.*, 2000, **201**, 2811.
15 Y. Lu, Y. Mei, M. Ballauff and M. Drechsler, *J. Phys. Chem. B*, 2006, **110**, 3930.
16 Y. Mei, Y. Lu, F. Polzer, M. Ballauff and M. Drechsler, *Chem. Mater.*, 2007, **19**, 1062.
17 Y. Wang, G. Wei, W. Zhang, X. Jiang, P. Zheng, L. Shis and A. Dong, *J. Mol. Catal. A -Chem*, 2007, **266**, 233.
18 D. Li, J. R. Dunlap and B. Zhao, *Langmuir*, 2008, **24**, 5911.
19 X. Jiang, B. Wang, C. Y. Li and B. Zhao, *J. Polym. Sci. A1*, 2009, **47**, 2853.
20 N. Pradhan, A. Pal and T. Pal, *Colloid Surface A*, 2002, **196**, 247.
21 S. K. Ghosh, M. Mandal, S. Kundu, S. Nath and T. Pal, *Appl. Catal. A-Gen.*, 2004, **268**, 61.
22 S. Wunder, F. Polzer, Y. Lu, Y. Mei and M. Ballauff, *J. Phys. Chem. C*, 2010, **114**, 8814.
23 S. Minko, S. Patil, V. Datsyuk, F. Simon, K. Eichhorn, M. Motornov, D. Usov, I. Tokarev and M. Stamm, *Langmuir*, 2002, **18**, 289.
24 C. Werner, K.-J. Eichhorn, K. Grundke, F. Simon, W. Grählert and H.-J. Jacobasch, *Colloids Surf., A*, 1999, **156**, 3.
25 K. Swaminatha Iyer, B. Zdyrko, H. Malz, J. Pionteck and I. Luzinov, *Macromolecules*, 2003, **36**, 6519.
26 E. Palik, *Handbook of Optical Constants of Solids II: 2*, Academic Press Inc., Boston, MA, 1991.

27 P. Müller-Buschbaum, *Anal. Bioanal. Chem.*, 2003, **376**, 3.

28 S. Roth, R. Döhrmann, M. Dommach, M. Kuhlmann, I. Kröger, R. Gehrke, H. Walter, C. Schroer, B. Lengeler and P. Müller-Buschbaum, *Rev. Sci. Instr.*, 2006, **77**, 085106.

29 P. Müller-Buschbaum, N. Hermsdorf, S. V. Roth, J. Wiedersich, S. Cunis and R. Gehrke, *Spectrochim. Acta B*, 2004, **59**, 1789.

30 M. A. Mangold, M. A. Niedermeier, M. Rawolle, J. Perlich, S. V. Roth, A. W. Holleitner and P. Müller-Buschbaum, *Phys. Status Solidi R*, 2011, **5**, 16.

31 G. Vineyard, *Physical Review B*, 1982, **26**, 4146.

32 R. Hosemann, W. Vogel, D. Weick and F. Balta-Calleja, *Acta Crystallographica, Sectian A*, 1981, **37**, 85.

33 J. Roda, *Makromol. Chem.*, 1977, **178**, 203.

34 C.-W. Chen and M. Akashi, *Langmuir*, 1997, **13**, 6465.

35 S. Burkert, E. Bittrich, M. Kuntzsch, M. Müller, K.-J. Eichhorn, C. Bellmann, P. Uhlmann and M. Stamm, *Langmuir*, 2010, **3**, 1786.

36 H. G. Schild, *Prog. Polym. Sci*, 1992, **17**, 163.

37 M. Heskins and J. E. Guillet, *J. Macromol. Sci. -Chem.*, 1968, **2**, 1441.

38 W. Wang, K. Troll, G. Kaune, E. Metwalli, M. Ruderer, K. Skrabania, A. Laschewsky, S. V. Roth, C. M. Papadakis and P. Müller-Buschbaum, *Macromolecules*, 2008, **41**, 3209.

39 W. Wang, E. Metwalli, J. Perlich, C. M. Papadakis, R. Cubitt and P. Müller-Buschbaum, *Macromolecules*, 2009, **42**, 9041.

40 W. Wang, G. Kaune, J. Perlich, C. M. Papadakis, A. M. B. Koumba, A. Laschewsky, K. Schlage, R. Röhlsberger, S.V.Roth, R. Cubitt and P. Müller-Buschbaum, *Macromolecules*, 2009, **42**, 9041.

41 E. B. Zhulina, O. V. Borisov, V. A. Pryamitsyn and T. M. Birshtein, *Macromolecules*, 1991, **24**, 140.

42 P. Auroy and L. Auvray, *Macromolecules*, 1992, **25**, 4134.

43 J. Habicht, M. Schmidt, H. Rühe and D. Johannsmann, *Langmuir*, 1999, **15**, 2460.

44 E. Bittrich, S. Burkert, M. Müller, K.-J. Eichhorn, M. Stamm and P. Uhlmann, *Langmuir*, 2012, **28**, 3439.

45 S. Minko, M. Müller, D. Usov, A. Scholl, C. Froeck and M. Stamm, *Phys. Rev. Lett.*, 2002, **88**, 035502.

46 M. Müller, *Phys. Rev. E*, 2002, **65**, 030802.

47 S. Arrhenius, *Z. Phys. Chem.*, 1889, **4**, 226.